NATIONAL AERONAUTICS AND SPACE ADMINISTRATION

Technical Report 32-1190

Digital Computer Analysis and Design of a Subreflector of Complex Shape

A. Ludwig

W. V. T. Rusch

JET PROPULSION LABORATORY
CALIFORNIA INSTITUTE OF TECHNOLOGY
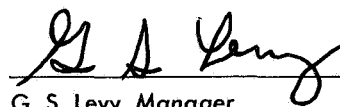PASADENA, CALIFORNIA

November 15, 1967

NATIONAL AERONAUTICS AND SPACE ADMINISTRATION

Technical Report 32-1190

Digital Computer Analysis and Design of a Subreflector of Complex Shape

A. Ludwig

W. V. T. Rusch

Approved by:

G. S. Levy, *Manager*
Communications Elements Research Section

JET PROPULSION LABORATORY
CALIFORNIA INSTITUTE OF TECHNOLOGY
PASADENA, CALIFORNIA

November 15, 1967

TECHNICAL REPORT 32-1190

Acknowledgment

Contents

Figures

Abstract

A technique for computing the scattered pattern of a complex subreflector/illumination pattern combination is presented. Computed results are compared with both boundary value solutions and experimental data, and there is excellent agreement in both cases. Present and future applications of computed scattered patterns are also discussed.

Digital Computer Analysis and Design of a Subreflector of Complex Shape

I. Introduction

The optimization of antenna feed systems has become increasingly important with the advent of very large (and therefore very expensive) low-noise microwave antenna systems. Optimization problems are complex in Cassegrainian or two-reflector antennas, since diffraction effects occur at both the primary paraboloidal reflector and the secondary subreflector. An example of the complex interdependence of design parameters in a Cassegrainian system is the relationship between the edge illuminations of the subreflector and the main reflector. This relationship has important effects on antenna efficiency, noise temperature, and side-lobe performance.

For the purpose of developing design criteria for a two-reflector antenna system, a theoretical analysis of the scattering from a truncated surface of revolution has been carried out. This analysis is based on the vector Kirchhoff theory of physical optics. The resulting integral expressions are considerably simplified because axial symmetry obtains, and the azimuthal integrals reduce to Bessel functions. However, the remaining integrals are sufficiently complex to require numerical evaluation on a large digital computer.

A similar technique has been applied to the scattering of an axially symmetric wave from a hyperboloid (Ref. 1).

In the present report, the problem has been generalized to an arbitrary surface of revolution illuminated by an arbitrary wave. Although the shape of the reflector should be consistent with the conditions imposed by the approximations, there are instances where these conditions may be violated and still yield calculated results in good agreement with experimental data. In fact, confidence in the entire analysis is reinforced by consistently good agreement with experimental results, some of which are presented here. The analysis, thus confirmed, can then be utilized in various applications and design procedures.

II. Formulation of the Field Integrals

In terms of the geometry of Fig. 1, the incident electric field $\mathbf{E}_{PF}$ of the wave emerging from the primary feed horn at 0 may be described by

$$\mathbf{E}_{PF} = \frac{e^{-jk\rho}}{\rho} \left\{ \sum_m \left[a_m(\theta') \sin m\phi' + b_m(\theta') \cos m\phi' \right] \mathbf{a}_\theta' \right. $$
$$\left. + \sum_m \left[c_m(\theta') \sin m\phi' + d_m(\theta') \cos m\phi' \right] \mathbf{a}_\phi' \right\}$$

$$(1)$$

where the functions a_m, b_m, c_m, and d_m are, in general, complex. Equation (1) is a completely general expression

Fig. 1. System geometry

for any realizable far-field feed pattern. A simple example of the preceding general expression is the field of a linearly polarized feed horn:

$$\mathbf{E}_{PF} = \frac{e^{-jk\rho}}{\rho} \{a_1(\theta') \sin \phi' \, \mathbf{a}_{\theta'} + d_1(\theta') \cos \phi' \, \mathbf{a}_{\phi'}\} \qquad (2)$$

In Eq. (2), $a_1(\theta')$ represents the E-plane (yz-plane) pattern and $d_1(\theta')$ represents the H-plane (xz-plane) pattern. For reasons of continuity, it is necessary that $a_1(180$ deg$) = -d_1(180$ deg$)$.

The magnetic field of the primary feed horn can be simply derived in the far zone to be

$$\mathbf{H}_{PF} = \sqrt{\frac{\varepsilon_0}{\mu_0}} \; (\mathbf{a}_\rho \times \mathbf{E}_{PF}) \qquad (3)$$

It will be assumed that the axially symmetric subreflector can be described by the general polar equation

$$(k\rho) g(\theta') = -1 \qquad \theta_0 \leqq \theta' \leqq \pi \qquad (4)$$

where $k = \omega \sqrt{\mu_0 \varepsilon_0} = 2\pi/\lambda$. The function $g(\theta')$ is illus-

trated below for several specific conic functions of revolution:

Sphere of radius a, centered at 0:

$$g(\theta') = -\frac{1}{ka} \qquad (5)$$

Paraboloid of focal length f with focus at 0:

$$g(\theta') = \frac{\cos \theta' - 1}{2 kf} \qquad (6)$$

Hyperboloid or ellipsoid of eccentricity e, semifocal distance c, and one focus at 0:

$$g(\theta') = \frac{(1 + e \cos \theta')}{kec\left(1 - \dfrac{1}{e^2}\right)} \qquad (7)$$

Disc coaxial with the z-axis located at $z = -d$:

$$g(\theta') = \frac{\cos \theta'}{kd} \qquad (8)$$

The vector Kirchhoff integral theory of physical optics (current-distribution method) may then be used to determine the field scattered from the subreflector. To approximate the surface currents it is assumed that local reflection occurs optically, thus requiring the wavelength of the incident field to be much smaller than the characteristic dimensions and radii of curvature of the subreflector. The radius of curvature of the incident spherical wavefront is also required to be much larger than a wavelength. The resulting analytical expressions, which are considerably simplified as a result of the axial symmetry of the primary feed fields and the subreflector, are

$$\mathbf{E}_s = \frac{e^{-jkR}}{R} \left\{ \sum_m [f_m(\theta) \sin m\phi + g_m(\theta) \cos m\phi] \, \mathbf{a}_\theta + \sum_m [h_m(\theta) \sin m\phi + k_m(\theta) \cos m\phi] \mathbf{a}_\phi \right\} \tag{9}$$

where

$$f_m(\theta) = \left(-\frac{1}{2}\right)(j)^m \int_{\theta_0}^{\pi} \frac{d\theta' \, e^{-j\alpha} \sin \theta'}{[g(\theta')]^2} \{a_m(\theta') \big[\cos \theta \, [g'(\theta') \sin \theta' - g(\theta') \cos \theta'] \, [J_{m-1}(\beta) - J_{m+1}(\beta)]$$

$$- 2j \, [g'(\theta') \cos \theta' + g(\theta') \sin \theta'] \sin \theta \, J_m(\beta)\big] + d_m(\theta') \, [-g(\theta')] \cos \theta \, [J_{m-1}(\beta) + J_{m+1}(\beta)] \} \tag{10}$$

$$g_m(\theta) = \left(-\frac{1}{2}\right)(j)^m \int_{\theta_0}^{\pi} \frac{d\theta' \, e^{-j\alpha} \sin \theta'}{[g(\theta')]^2} \{b_m(\theta') \big[\cos \theta \, [g'(\theta') \sin \theta' - g(\theta') \cos \theta'] \, [J_{m-1}(\beta) - J_{m+1}(\beta)]$$

$$- 2j \, [g'(\theta') \cos \theta' + g(\theta') \sin \theta'] \sin \theta \, J_m(\beta)\big] + c_m(\theta') \, g(\theta') \cos \theta \, [J_{m-1}(\beta) + J_{m+1}(\beta)] \} \tag{11}$$

$$h_m(\theta) = \left(\frac{1}{2}\right)(j)^m \int_{\theta_0}^{\pi} \frac{d\theta' \, e^{-j\alpha} \sin \theta'}{[g(\theta')]^2} \{b_m(\theta') \, [g'(\theta') \sin \theta' - g(\theta') \cos \theta'] \, [J_{m-1}(\beta) + J_{m+1}(\beta)]$$

$$+ c_m(\theta') \, g(\theta') \, [J_{m-1}(\beta) - J_{m+1}(\beta)] \} \tag{12}$$

$$k_m(\theta) = \left(-\frac{1}{2}\right)(j)^m \int_{\theta_0}^{\pi} \frac{d\theta' \, e^{-j\alpha} \sin \theta'}{[g(\theta')]^2} \{a_m(\theta') \, [g'(\theta') \sin \theta' - g(\theta') \cos \theta'] \, [J_{m-1}(\beta) + J_{m+1}(\beta)]$$

$$- d_m(\theta') \, g(\theta') \, [J_{m-1}(\beta) - J_{m+1}(\beta)] \} \tag{13}$$

where

$$\alpha = \frac{\cos \theta' \cos \theta - 1}{g(\theta')} \tag{14}$$

$$\beta = \frac{-\sin \theta \sin \theta'}{g(\theta')} \tag{15}$$

Equations (9)–(13) have been programmed for numerical integration on a large digital computer. The major restriction imposed by the computer evaluation is the allowable machine time, which is a function of the number of field points and the size of the subreflector in wavelengths. For typical subreflectors of the order of 10–50 wavelengths in diameter, IBM 7094 machine time necessary to compute E- and H-plane patterns is generally between 10 and 30 min. A description of the computer program input/output is given in Ref. 2. The program limits the calculation to a maximum of $m = 4$ in Eq. (9). However, in many cases of interest, the $m = 1$ case alone is sufficient.

III. Applications

A. Feed System Design and Optimization

Since computed patterns may be generated relatively fast and inexpensively, many different feed pattern/subreflector combinations for Cassegrainian antennas may be evaluated. For example, in a recent application (Ref. 3), the beamwidth of a primary feed pattern was varied, and the resulting scattered patterns from a given subreflector were evaluated for illumination efficiency and spillover contributions to antenna noise temperature. Similarly, subreflector geometry may be varied parameter by parameter (e.g., edge angle, eccentricity, etc.) to determine optimum designs. This is particularly useful for subreflectors that are not purely hyperboloidal (for example, those with a conical flange, Ref. 4), since there are many variable parameters in this type of design. The value of existing or potential shaped-beam feeds for Cassegrainian systems (Ref. 5) is also readily determined.

Computed patterns have also been used to evaluate vertex plate designs. Typically, vertex plates not only produce a null on axis, but also perturb the entire scattered pattern (particularly for very low VSWR designs). The computed fields can be easily evaluated for decrease in returned power and for change in illumination efficiency. Theoretically, small vertex plates with sharp edges violate some of the assumptions made earlier, and the validity of the computed patterns is somewhat questionable in this application. However, there are indications (some of which will be presented later in this report) that the computations are better than one would expect. Unfortunately, the experimental verification of this application is very difficult. Measured patterns are perturbed by primary feed blockage (see Sec. IV), and measured returned power also includes horn mismatches and, in some cases, scattering from subreflector support struc-tures. The single attempt to experimentally verify a computed design was inconclusive because of these effects, but the combination of computation and experimentation led to an excellent design (which differed only slightly from the computed design) as an end result.[1] At the very least, the computed data sharply reduced the number of possible designs and shortened the experimental effort considerably.

B. Evaluation of Special Reflector Shapes

There has been substantial recent activity in the synthesis of Cassegrainian antennas with special reflector shapes to provide very high antenna efficiency (Refs. 6–8).

In the case of Potter's technique (Ref. 6), the synthesized subreflector is infinite, and patterns computed by the techniques of the present report may be used to evaluate the effect of truncation (see Sec. IV). Also, the feed pattern synthesized by this technique is complex in shape and the effect of using a somewhat different, but realizable, feed pattern may be determined.

The synthesis technique developed by Galindo (Ref. 7) is based on geometrical optics, and computed patterns may be used to evaluate the effect of diffraction. The fields scattered from the subreflector may in turn be used as input illumination to determine the pattern of the main reflector, resulting in an overall evaluation of the system for a given configuration and wavelength. This latter application is the subject of a current investigation at the Jet Propulsion Laboratory (JPL), with only preliminary results available at this time (Ref. 9). Figure 2, for example, shows computed scattered fields from such a subreflector with a diameter of 40 wavelengths. Even for a subreflector of this size, diffraction effects are important and must be considered in a design based on this technique.

C. Gain and Noise Temperature Predictions

Computed patterns are useful not only for optimizing feed system designs; in addition, the gain and antenna noise temperature predictions for final designs based on computed patterns have proved quite accurate. In one case, a 30-ft-diameter antenna, operating at S-band, used a subreflector with a large vertex plate that severely distorted the illumination pattern. Predicted gain, including the loss due to aperture blockage, was 42.6 dB (45% efficiency). Measured gain was 42.2 ±0.5 dB.[1] In a recent application, the gain of the NASA/JPL 210-ft-diameter

---

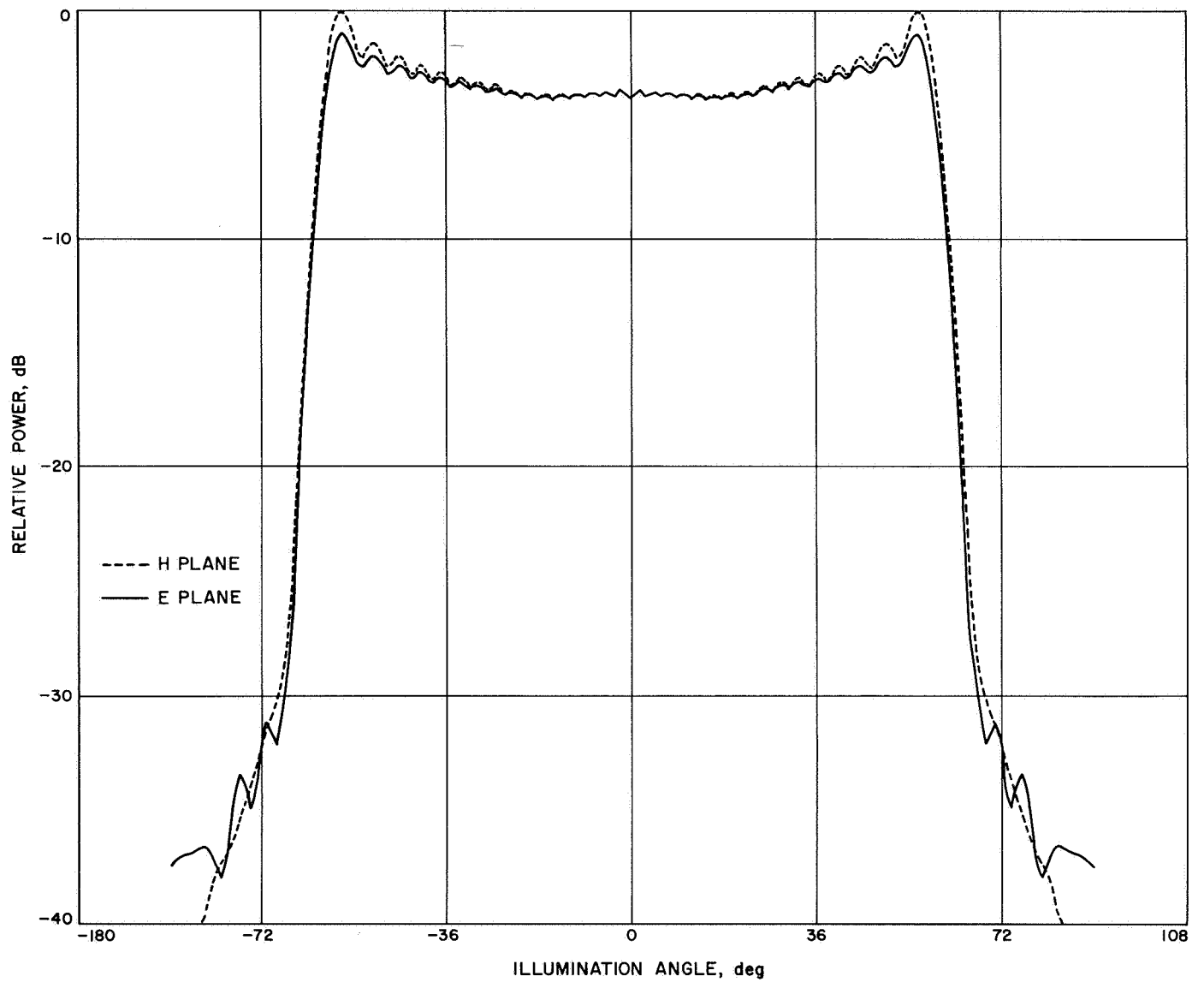[1]Hartop, R., private communication, 1966.

Fig. 2. Computed scattered fields from a subreflector synthesized by a geometrical optics technique

antenna, operating at S-band, was predicted to be 61.90 + 0.19 − 0.17 dB (65.3% efficiency), including loss due to aperture blockage and surface tolerance (Ref. 10). Measured gain was 61.9 ±0.7 dB (Ref. 11). Predicted antenna noise temperatures for this case also agreed very well with measured values (Ref. 11).

IV. Experimental and Theoretical Verification of Computed Results

A. Comparison With Boundary Value Solution

The antenna synthesis technique developed by Potter (Ref. 6) includes an iterative boundary value solution of a feed pattern and reflector required to produce a specific far-field pattern. The reflector is infinite, but the illumination drops off rapidly outside a finite angular region. One would expect that truncating the reflector at a point where the illumination is very low would have very little

Fig. 3. Subreflector synthesized by Potter's technique

effect on the resulting scattered pattern. Although the reflector generally follows the shape of a hyperboloid, in detail the shape is complex, as shown in Fig. 3. The feed pattern is also complex in shape, as shown in Fig. 4, and the combination provides a rigorous test for a numerical scattering program. A comparison of computed patterns and the boundary value solutions has been published previously (Ref. 12). Recently, more detailed data have been obtained. Figure 5 illustrates two such cases, where scattering was computed for a pattern/reflector combination synthesized by Potter's method. The second case corresponds to the system illustrated in Figs. 3 and 4; the first case represents a similar configuration, but without a vertex plate type area in the center. There is excellent agreement between the pattern expected from the boundary value solution and the numerically computed pattern. The minor discrepancies are almost certainly due to the effects of truncation. (As the subreflector is extended, the agreement definitely improves.) The second case shown in Fig. 5, where a hole has been synthesized in the center of the pattern, provides the strongest evidence that the computed patterns are valid for subreflectors with vertex plates. The agreement in the phase patterns is also remarkably good in this case.

Although both solutions presented in these figures are basically theoretical, they are almost totally independent in technique, and the excellent agreement provides strong confidence in both methods.

B. Comparison With Experimental Pattern

Experimental patterns have been compared with computed patterns for subreflector diameters of 7.8, 19.5, and 28.4 wavelengths in a previous report (Ref. 1). Agreement was good in all cases, even though the feed pattern was approximated by a circularly symmetric composite pattern with uniform phase. More recent experimental and computed data have been obtained for a subreflector of 51.3 wavelengths in diameter, consisting of a hyperboloid with a conical flange extension, as shown in Fig. 6. The experimental feed-horn pattern is shown in Fig. 7. In this case, detailed E- and H-plane amplitude and phase information (not circularly symmetric) was the input to the computer program.

Figure 8 illustrates the geometry for the experimental pattern measurement; the operating frequency was 16 GHz, and a serrodyne system was used for amplitude and phase measurements. Experimental and computed E-plane amplitude and phase patterns are shown in
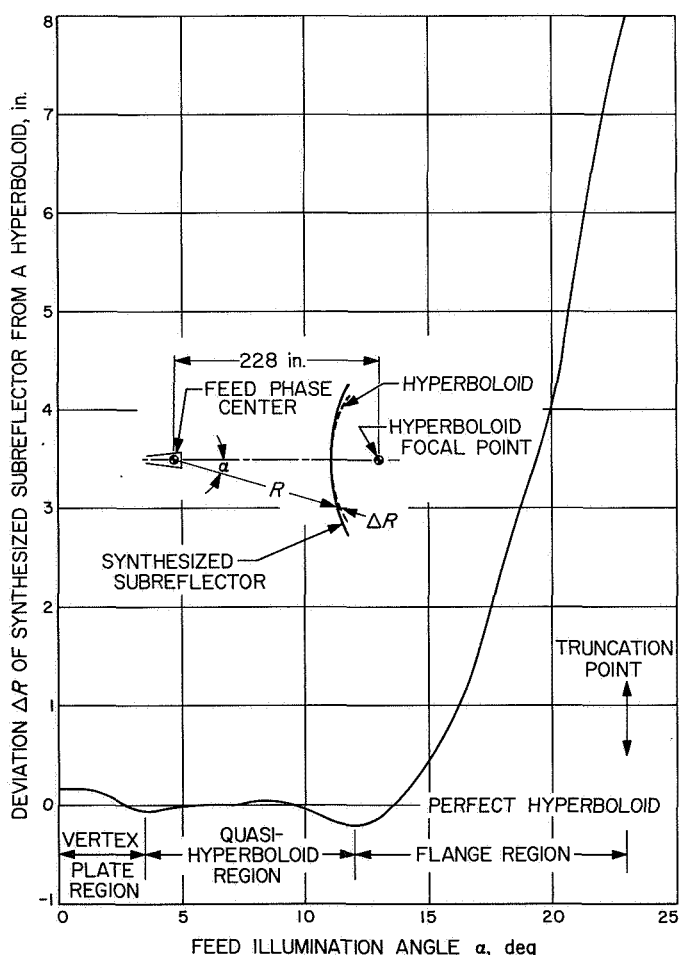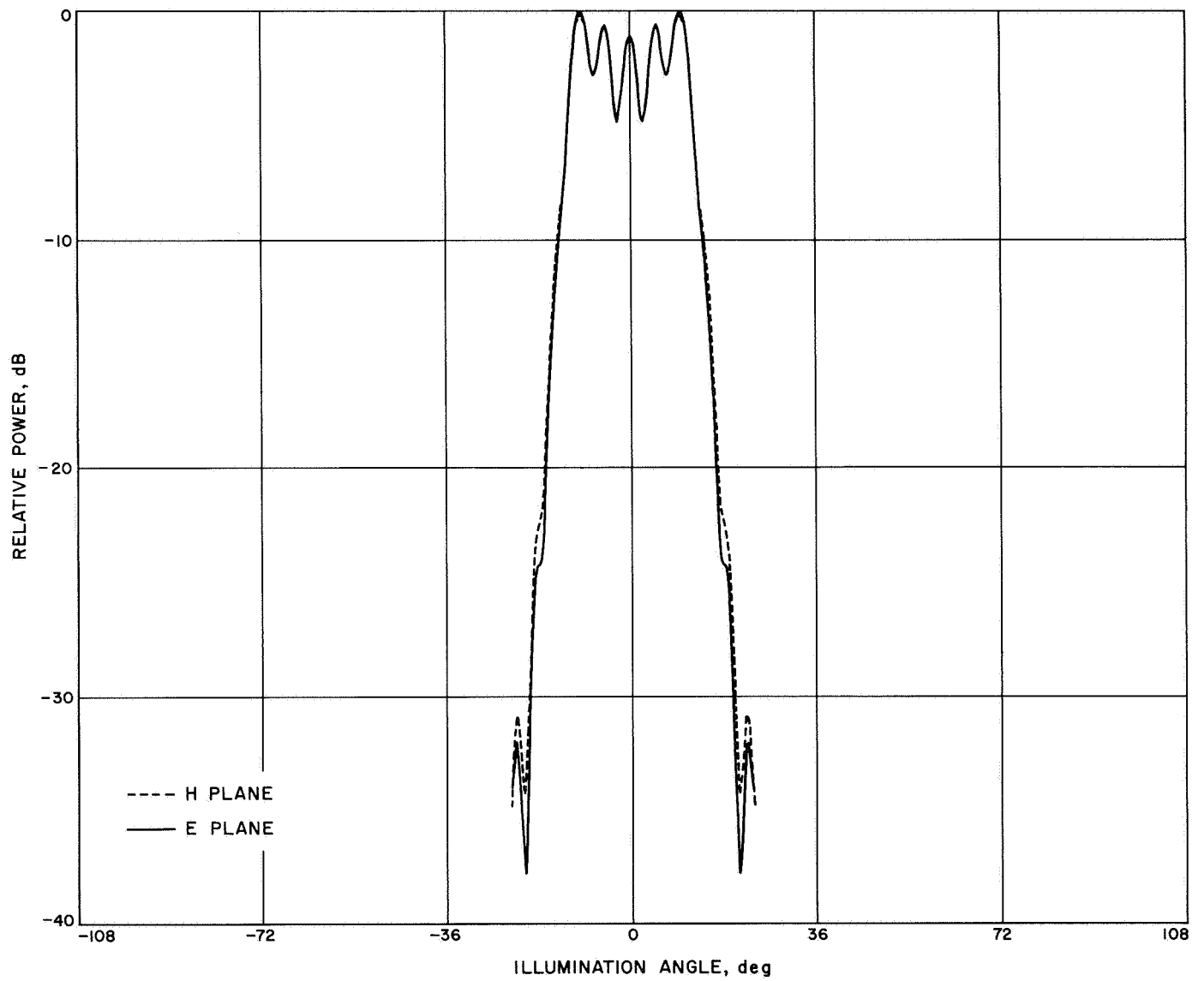
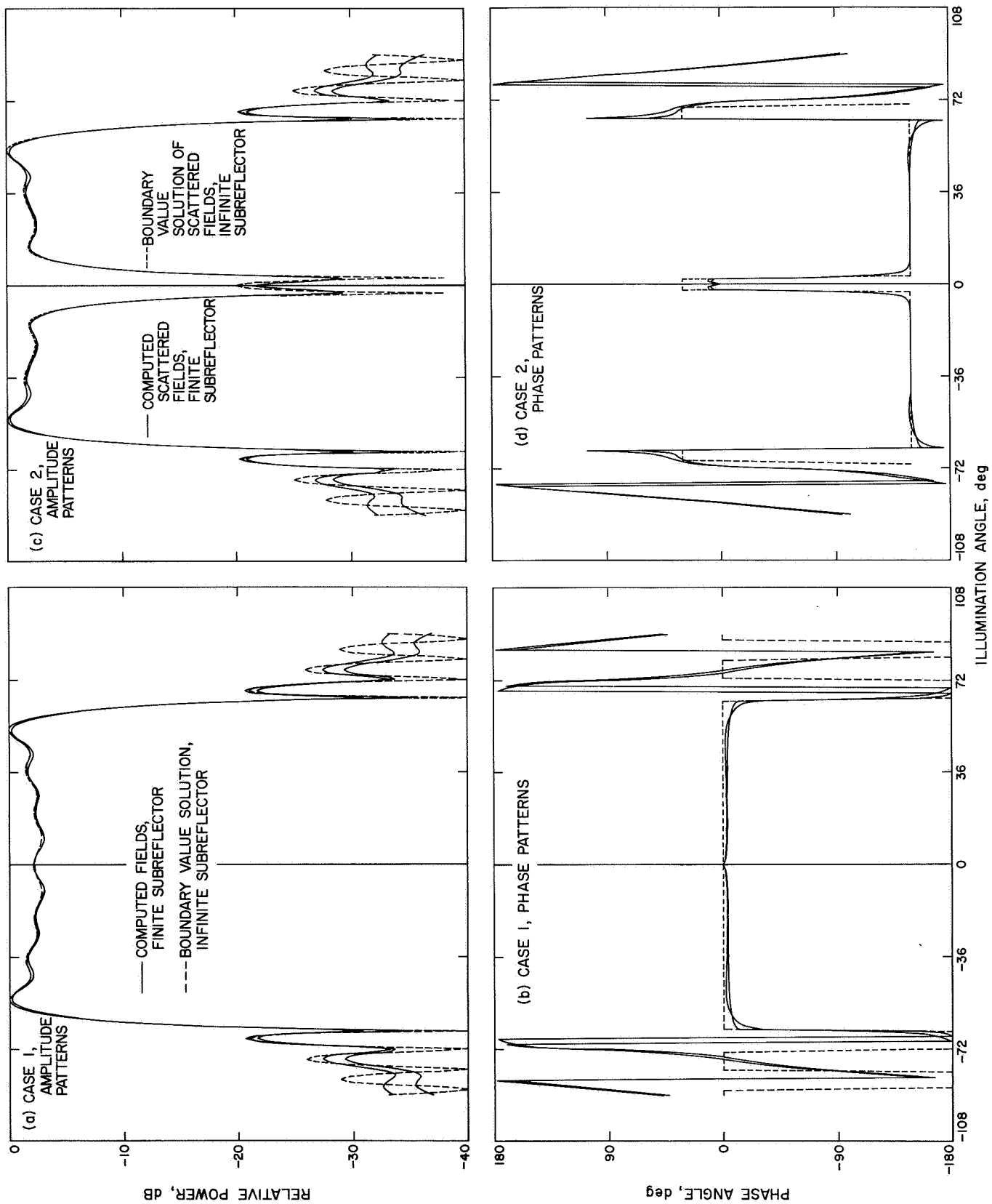Fig. 4. Feed pattern synthesized by Potter's technique

Fig. 5. Comparison of computed scattered fields with boundary value solution: (a) case 1, amplitude patterns, (b) case 1, phase patterns, (c) case 2, amplitude patterns, (d) case 2, phase patterns
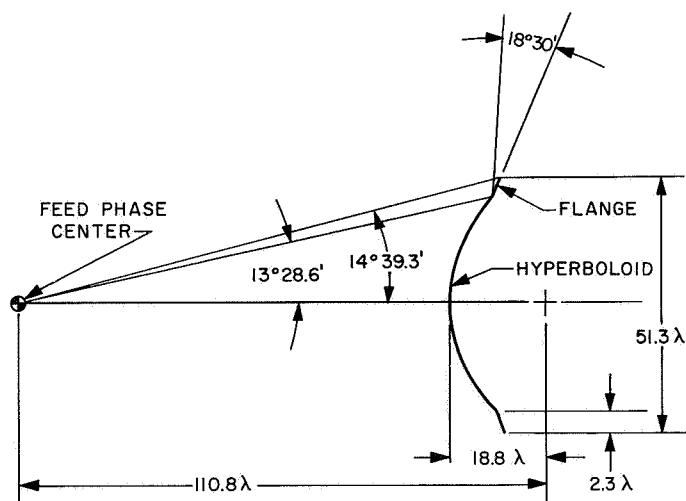
Fig. 6. Subreflector configuration for experimental scattered patterns

Fig. 9; the H-plane patterns are very similar in both cases. The discrepancy on axis (0 deg) is due to blockage by the feed horn, and the disagreement in the spillover region (140–180 deg) is due to the parallax inherent in the short antenna range shown in Fig. 8. This is due to the fact that the computed results correspond to an infinite antenna range, where the angle and distance from an observation point to the subreflector focus and primary feed focus are virtually equal. For a finite range this is not true. In Fig. 8 the center of rotation is about the subreflector focus, and the indicated angle is correct for fields diverging from this point; the indicated angle is not correct for fields diverging from the feed focus. Unfortunately the range distance for this case is not known exactly, but scaling from Fig. 8 and applying a geometrical correction for angle and distance (which affects "space loss"), we find that the experimental pattern agrees well (within 1.7 dB and 3 deg of angle) with the computed pattern, in the spillover region.

The reason for the disagreement on the steep portion of the pattern (62–68 deg) is not completely clear. A parallax effect similar to that discussed above may be partially responsible. Also, there is a significant amplitude and phase taper across the aperture of the probe antenna (considering it as a receiving horn), and although an

analysis indicates that this taper would introduce only a small error, it is a contributing factor. It is also conceivable that a primary feed-horn side lobe below −40 dB (feed-horn fields below −40 dB were neglected in the computer's pattern) is causing destructive interference in this region; the behavior of the first side lobe in the experimental scattered pattern supports this possibility to some extent. The scattered fields in this region are particularly dependent on the behavior at the edge of the subreflector, and one would expect some error in the computed pattern, because of edge effects; this appears to be the most likely explanation for the major portion of the discrepancy.

The remaining minor differences in other portions of the pattern could be partially caused by (1) errors in the computed patterns, due to inexact input data, finite integration step size, or the second-order effects of reflector curvature, or (2) other experimental problems such as ground reflections, boresight errors, and detector nonlinearities.

In any case, we are in the fortunate position of worrying about relatively minor discrepancies, since the overall agreement is excellent. The good agreement between experimental and computed phase patterns is particularly satisfying, since phase variations are typically more difficult to compute accurately and are also much more difficult than amplitude patterns to measure experimentally.

Originally the primary value of computed patterns was thought to be a quick and easy method for approximately evaluating many feed system configurations, which would be a difficult and time-consuming task experimentally. However, the agreement obtained between calculated and experimental patterns stimulated a careful analysis of experimental errors, and it became clear that in many ways the computed patterns are more accurate. In current practice, the computed patterns are used for final predictions of feed system performance. Actually the difference in performance predictions is very small either way, and perhaps the major reason for using computed results is the convenience of using computer data versus the tedious effort of measuring and reducing experimental patterns.
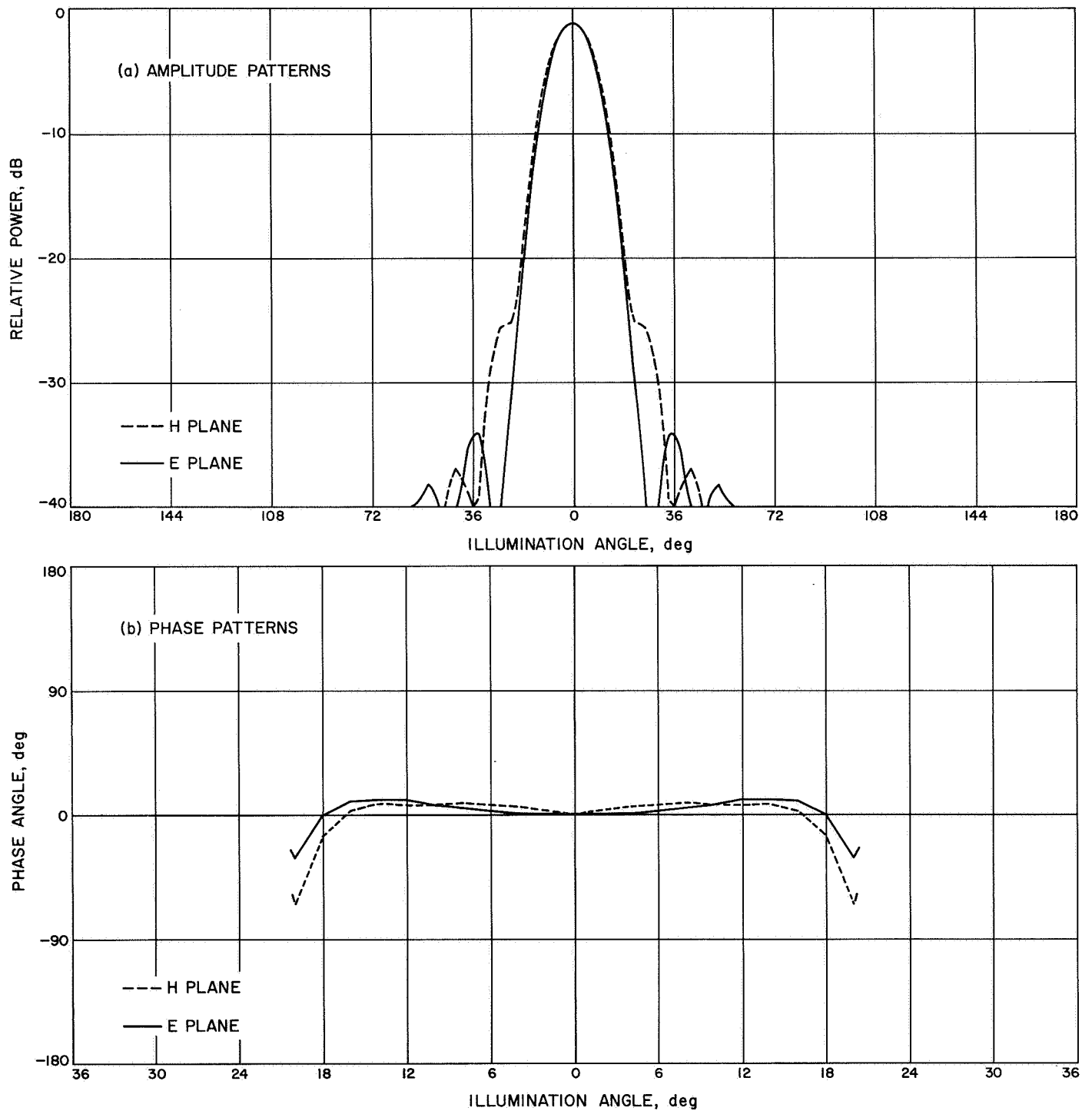
Fig. 7. Primary feed pattern for experimental scattered patterns: (a) amplitude patterns, (b) phase patterns
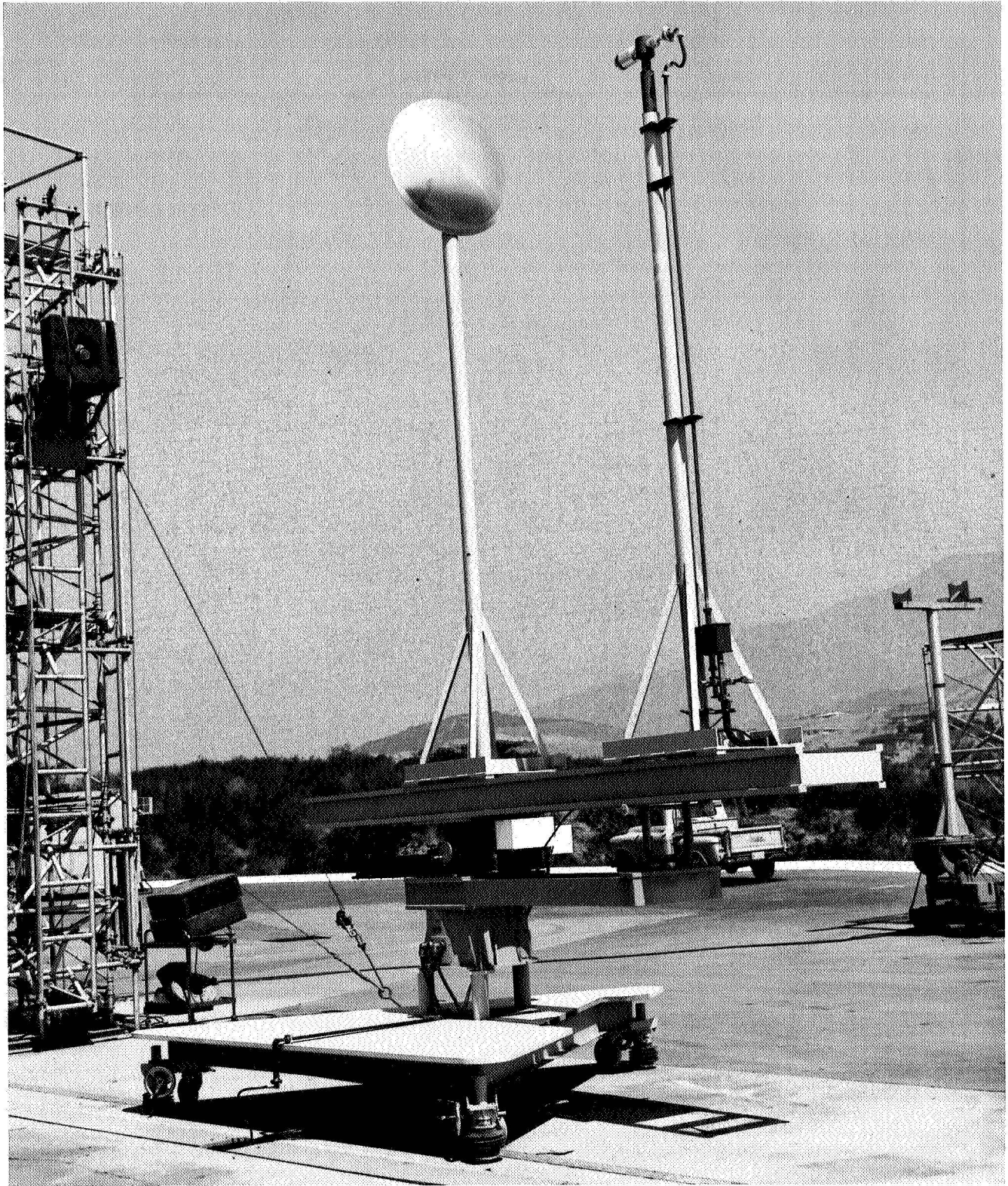
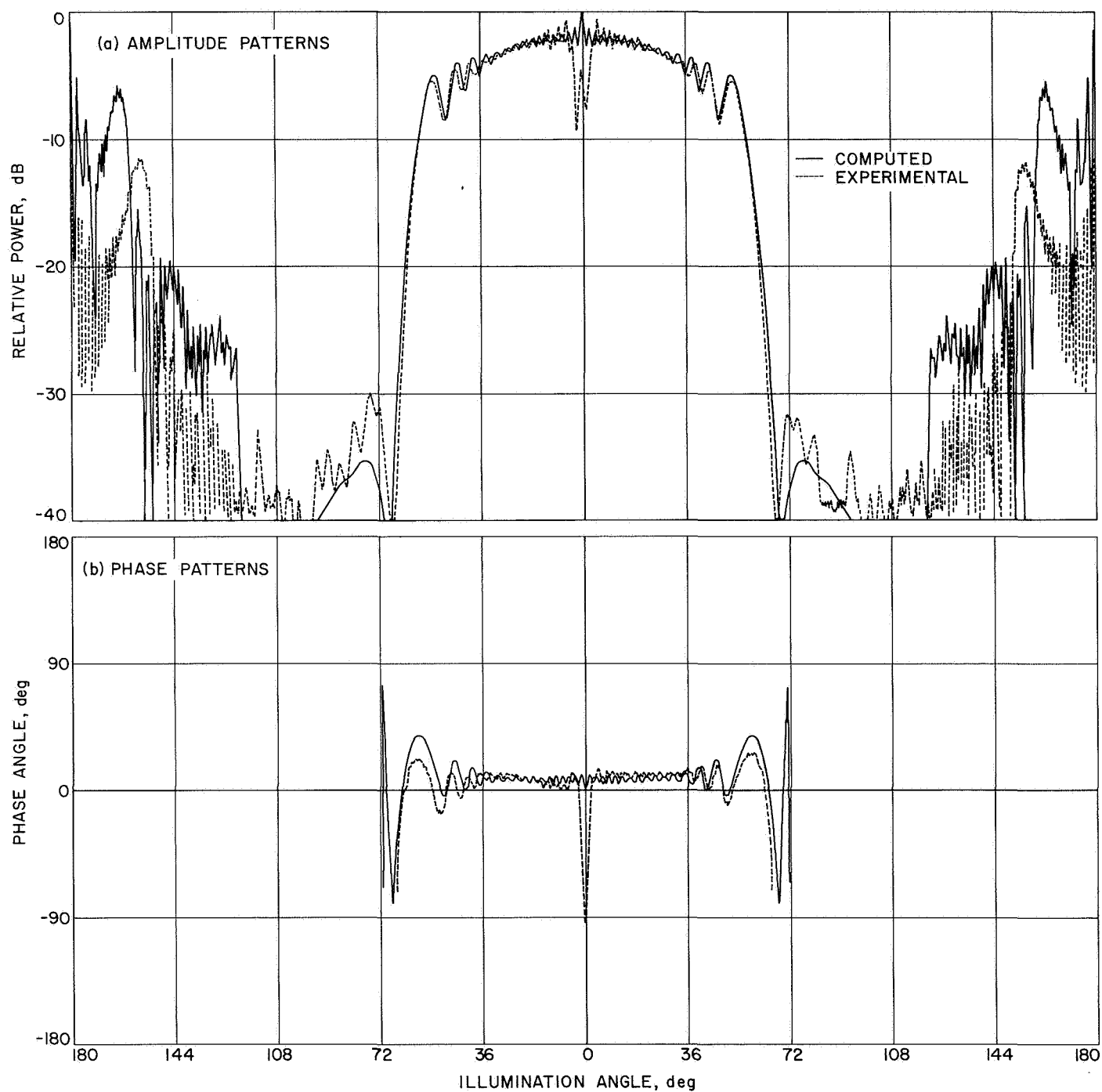Fig. 8. Antenna range for experimental scattered patterns

Fig. 9. Comparison of computed and experimental scattered fields: (a) amplitude patterns, (b) phase patterns

References

1. Rusch, W. V. T., "Scattering From a Hyperboloidal Reflector in a Cassegrainian Feed System," *IEEE Trans. Ant. Prop.*, Vol. AP-11, pp. 414–421, July 1963.

2. Ludwig, A., et al., *Computer Programs for Antenna Feed System Design and Analysis*, Technical Report 32-979, Sec. VI. Jet Propulsion Laboratory, Pasadena, Calif., Sept. 1966.

3. Ludwig, A., "Advanced Antenna System (AAS) Feed System Optimization," *Supporting Research and Advanced Development*, Space Programs Summary 37-34, Vol. IV, pp. 239–241. Jet Propulsion Laboratory, Pasadena, Calif., Aug. 1965.

4. Potter, P. D., "A Simple Beamshaping Device for Cassegrainian Antennas," Technical Report 32-214. Jet Propulsion Laboratory, Pasadena, Calif., Jan. 1962.

5. Ludwig, A., "Radiation Pattern Synthesis for Circular Aperture Horn Antennas," *IEEE Trans. Ant. Prop.*, Vol. AP-14, pp. 434–440, July 1966.

6. Potter, P. D., "Application of Spherical Wave Theory to Cassegrainian-Fed Paraboloids," to be published in *IEEE Trans. Ant. Prop.*

7. Galindo, V., "Design of Dual-Reflector Antennas With Arbitrary Phase and Amplitude Distributions," *IEEE Trans. Ant. Prop.*, Vol. AP-12, pp. 403–408, July 1964.

8. Williams, W. F., "High Efficiency Antenna Reflector," *Microwave J.*, pp. 79–82, July 1965.

9. Ludwig, A., "Shaped Reflector Cassegrainian Antennas," *Supporting Research and Advanced Development*, Space Programs Summary 37-35, Vol. IV, pp. 266–268. Jet Propulsion Laboratory, Pasadena, Calif., Oct. 1965.

10. Ludwig, A., "Calculated Gain of the Advanced Antenna System," *The Deep Space Network*, Space Programs Summary 37-42, Vol. III, pp. 37–40. Jet Propulsion Laboratory, Pasadena, Calif., Nov. 1966.

11. Potter, P. D., "Design and Performance of the NASA/JPL 210 Foot Steerable Paraboloid," presented at the British IEE Conference on Design and Construction of Large Steerable Aerials, London, England, June 1966.

12. Rusch, W. V. T., "Antenna Feed Research: Scattering of an Arbitrary Spherical Wave by an Arbitrary Surface of Revolution," *Supporting Research and Advanced Development*, Space Programs Summary 37-31, Vol. IV, pp. 286–287. Jet Propulsion Laboratory, Pasadena, Calif., Feb. 1965.